

Integration of high frequency piezoelectric transducer for lab-on-chip

J. Gao, Julien Carlier, S. Wang, Pierre Campistron, Dorothée Debavelaere-Callens, S. Guo, X. Zhao, Bertrand Nongaillard

▶ To cite this version:

J. Gao, Julien Carlier, S. Wang, Pierre Campistron, Dorothée Debavelaere-Callens, et al.. Integration of high frequency piezoelectric transducer for lab-on-chip. Acoustics 2012, Apr 2012, Nantes, France. paper 000480, 3323-3328. hal-00802625

HAL Id: hal-00802625

https://hal.science/hal-00802625

Submitted on 20 Mar 2013

HAL is a multi-disciplinary open access archive for the deposit and dissemination of scientific research documents, whether they are published or not. The documents may come from teaching and research institutions in France or abroad, or from public or private research centers.

L'archive ouverte pluridisciplinaire **HAL**, est destinée au dépôt et à la diffusion de documents scientifiques de niveau recherche, publiés ou non, émanant des établissements d'enseignement et de recherche français ou étrangers, des laboratoires publics ou privés.



Integration of high frequency piezoelectric transducer for Lab-On-Chip

J. Gao^a, J. Carlier^a, S. Wang^a, P. Campistron^a, D. Callens^a, S. Guo^b, X. Zhao^b and B. Nongaillard^a

^aIEMN-DOAE-UMR CNRS 8520, Avenue Poincaré - BP 60069 - 59652, 59650 Villeneuve D'Ascq, France

^bWuhan University, Physics department, Wuhan University, 430072 Wuhan, China pandagjm@msn.com

In this paper, we developed an integrated microsystem based on 1GHz longitudinal bulk waves which propagate inside silicon wafer. In order to develop high frequency acoustic wave characterization in Lab-On-Chip, a heterogeneous technology has been developed based on the use of silicon, silicon dioxide, ZnO, PDMS. Silicon based acoustic mirrors have been developed to guide the acoustic beam in a plane parallel to the surface of the substrate and through the microfluidic channel. Vertical mirrors not only guide the acoustic wave in the parallel plane, but also eliminate a part of the acoustic noise of the system.

1. Introduction

Acoustic wave technology and devices have been in commercial use in the past several decades [1]. Most acoustic wave devices can be used as sensors because they are sensitive to mechanical, chemical, or electrical perturbations on the surface of the device [2, 3]. Acoustic wave sensors have the advantage that they are versatile, sensitive, and reliable. They can detect not only mass/density changes, but also viscosity, elastic modulus, and have wide applications in monitoring of pressure, moisture, temperature, force, acceleration, shock, viscosity, flow, ionic contaminants, [4,5]. Recently, there has been an increasing interest in acoustic wave based biosensors to detect the traces of biomolecules (biomarkers) such as DNA, proteins (enzymes, antibodies, and receptors), cells and tissue (microorganisms, animal and plant cells, cancer cells etc.), biochemical substances or viruses [6-8].

In this article, we report a novel acoustic wave device based on the bulk acoustic wave (BAW) for sensing. BAW are generated by miniature ZnO piezoelectric transducers. They can be grown in thin film form on a variety of substrates, including silicon, making them perhaps the most promising material for integration. Because of non contact nature and the high resolution (1.5 micron resolution at GHz) of acoustic waves, the acoustic wave device would be useful for non destructive elastic characterization and detection of microscopic objects

2. Materials and methods

By means of the signal reflected on the mirror, a microsystem is designed for realizing the characterization of the chemical solution and detection of latex particles. It contains 45°mirrors, microchannel and piezoelectric transducers used as an emitter and receiver. A schematic view of the system without dimensions is presented in Fig.1. In order to realize the electrical matching and conversion

technology, the piezoelectric transducers were deposited on one side of the silicon wafer. The other micromachined components and the microfluidic channel structures were achieved on the other side of the wafer which was packaged with PDMS in order to provide an easy optical observation and manipulation.

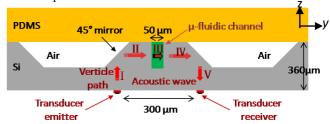


Fig 1. Schematic for transmission mode of the acoustic microsystem without vertical mirror

There are three important steps to fabricate the microsystem: mirror wet etching, microfluidic channel fabrication using deep reactive ion etching, and transducer sputtering. The fabrication process was shown in Fig 3.

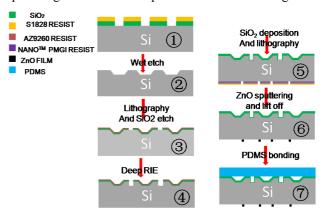


Fig 2. The flow chart of microsystem fabrication process

The reflection of an acoustic longitudinal wave upon a free surface in oblique incidence produces a mode conversion, so that there are reflected waves of both the longitudinal and shear polarizations [9]. It was reported that {1 1 0} silicon crystal planes fabricated by wet chemical etching could be used as 45° acoustic mirrors for reflecting acoustic beams. For acoustic waves, the reflection on a mirror led to a mode conversion from longitudinal to shear waves or from shear to longitudinal waves. The efficiency

of the reflection of the longitudinal wave could be improved by means of the deposition of a SiO_2 layer on the 45° mirror [10].

2.1 Microsystem fabrication

500nm SiO2 was deposited on both sides of a double-side polished silicon wafer (<100>, 370μm thick, 3 inches diameter) by Plasma Enhanced Chemical Vapor Deposition (PECVD) at 300° C. Using SiO₂ as the sacrifice layer, anisotropic aqueous TMAH and IPA mixed solution was performed to obtain smooth {110} plane 45° mirrors.

 $3.5~\mu m$ SIO2 were deposited on the 45° mirrors so as to limit the conversion mode of the acoustic wave from longitudinal wave to shear wave as presented in previous article [10]. Figure 3 shows the cross section images of microsystem obtained by Scanning Electron Microscopy (SEM). The width difference between the top and bottom microchannel is less 1%. The nearly 90° channel will not cause the mode conversion in the interface.

1 GHz piezoelectric transducers (Pt(100nm)/ZnO(2.4 μ m)/Pt(100nm)/Ti(10nm)) and metal were deposited on the other side of silicon wafer using radio frequency magnetron sputtering. The area of piezoelectric rectangle transducers is 200 m \times 100 m in order to ensure good electrical matching of the transducers (a real part of the impedance about 50Ω at the resonance frequency).

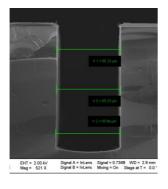


Fig 3. SEM image: cross section of microfluidic channel

3. Result and discussion

3.1 Signal processing

Electrical measurements using network analyzers are of common use in RF electronics characterizations. Their major interest is the low level of noise (-110dBm).

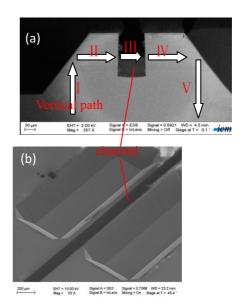
Here we measure the $S_{ij}(i,j=1 \text{ or } 2)$ scattering parameter defined as the ratio of the complex amplitudes of the

reflected and transmitted to the incident voltage thanks to a Suss Microtech prober on PM8 manual probe system (CASCADE MICROTECH) coupled with a ROHDE&SCHWARZ ZVA8 Vector Network Analyzer. It has been shown that this parameter is composed of two terms, a purely electrical one, and an acoustical one [3]: $S_{ij}(f) = S_{ij}^{elect} \cdot + KS_{ij}^{acoust} \cdot \cdot .$

The origin of the electrical term is due to the reflection of the electrical wave on the transducer. This term vanishes if the transducer is perfectly electrically matched to the impedance of the line. The second term represents the acoustic wave propagating in the silicon wafer, and so on, reconverted by the transducer to an electrical signal. The network analyzer is calibrated in the plane of the transducer which provides us a phase or time origin. The inverse Fourier transform of the S_{ij} parameter can be interpreted as the impulse response of the system. In the time domain, the two terms of S_{ij} are separated. The electrical term occurs just after the origin of time and the acoustical one is delayed by the acoustic propagation time.

3.2 Acoustics measurements through microfluidic channel with and without EDI water

The thickness of the Silicon wafer is about $360\mu m$. The distance between the top of the mirrors and between the backside transducers is separately about $280\mu m$ and $290\mu m$. The width of the microchannel is $50\mu m$. The velocity of longitudinal acoustic wave is 8432m/s and the velocity of shear wave is 5398m/s. It is observed that there are longitudinal and shear waves propagated on this vertical path, also see fig. 1. A continuously sinusoidal wave was used as excitation. The central frequency of the ZnO transducers was characterized as about 1.3 GHz.



observed.

Fig4. The scheme of the microsystem: a. cross section of the SEM image of microsystem b. top view of the SEM image of the Si microsystem.

Fig 5 shows the comparison of S_{ij} magnitude spectra in

the case there is deionized water in the microfluidic channel and in the case it is empty. The data evaluate whether and when the acoustic wave transmitted through the microchannel. There are five section of path of the acoustic beam in the microsystem (fig 1). The sections of the acoustic path of transmission signal are labeled in fig 1 (path I-path V). L and S means longitudinal acoustic wave and shear wave, respectively. Using the Snell law $\frac{\sin\theta_i}{v_i} = \frac{\sin\theta_r}{v_r} \text{ can obtain the directions of the wave vectors}$ of acoustic waves. (v_i the velocity of the incident wave and θ_i the incident angle, v_r the velocity of the reflected wave, which can support longitudinal or shear polarization, and θ_r the reflected angle). The longitudinal wave is deflected by 90° on the 45° mirror ($i=45^\circ$) and the shear wave cannot

be converted on the second 45° mirror depending on the

Snell law[11]. So only LLLLS and LLLLL signals can be

The impulse response S_{21} presents several pulses which can be classified corresponding to the time of flight in the system as shown in fig 1. LLLLL represents that the longitudinal acoustic wave emitted by the transducer was reflected twice on the 45° mirror before reached the receptor. During the twice reflections, the longitudinal wave went through the microchannel when it is filled with water. In fig 5, we hardly distinguish the transmission signal comparing two situations in the microchannel. With empty channel the theoretical amplitude of this transmitted peak for S₂₁ transmission should be zero, because of the acoustic parasitic noise, the amplitude of $\,S_{21}\,$ transmission signal is evaluated at 1.46×10⁻⁴ for LLLLL while for the channel full with deionized water the amplitude of the peak is 1.63×10^{-4} . The signal to noise ratio is approximately equal to 1.1, which is very low for the further application.

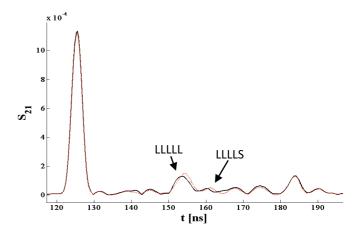
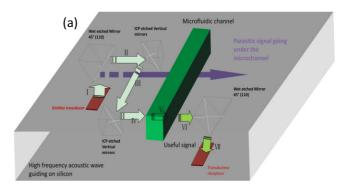


Fig 5 Real part of the impulse response of the system vs. time (ns): S_{21} , (red curve: channel full with EDI water; black curve: empty channel)

3.3 Improvement of vertical mirror

addition

Integration of the vertical mirrors in the silicon based microsystem can void deflection and acoustic wave propagation which go through the under the microchannel. It can strongly reduce the system acoustic parasitic noise and improve the signal to noise ratio. We introduced a pair of vertical mirrors between 45° mirror and microchannel, as shown in Fig 6.





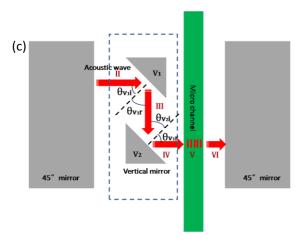


Fig 6: schematic of microsystem with the vertical mirrors (a) top view of the microsystem, (b) SEM image of the vertical mirror and the microchannel. (c) Top view of the microsystem.

The longitudinal velocity v_i in the $\{0\ 0\ 1\}$ direction is the same as v_r in the $\{0\ 1\ 0\}$ direction $(v_i = 8432\ m/s)$, the longitudinal wave reflection angle is 45°. The shear wave is in different situation, by the Snell law reflection angle of shear wave is 27° (θ_{rs}) and velocity is 5398 m/s. A thin silicon oxide layer deposited on the mirror can improve the efficiency of the reflection of the longitudinal wave. The same situation of conversion mode also happened on the pair of vertical mirror surface. The Snell equation on the surface vertical two $\frac{\sin\,\theta_{v_1i}}{v_{1i}} = \frac{\sin\,\theta_{v_1r}}{v_{1r}} \ \text{ and } \frac{\sin\,\theta_{v_2i}}{v_{2i}} = \frac{\sin\,\theta_{v_2r}}{v_{2r}} \ \ (\ v_1\ , \ \ v_2\ separately$ represents the first vertical mirror and second vertical mirror), because reflection interfaces of vertical mirrors are parallel, $\theta_{v_2i} = \theta_{v_1r}$ and $v_{1r} = v_{2i}$. We can obtain the equation $\frac{\sin \theta_{v_1 i}}{v_{1 i}} = \frac{\sin \theta_{v_2 r}}{v_{2 r}}$, the direction of acoustic wave reflected by the second vertical mirror is only concerned with the incidence direction of first vertical mirror and speed ratio: $\frac{v_{2r}}{v_{1i}}$. The direction of the shear energy propagation is given by the Poynting vector which is normal to the slowness curve. Using the Snell law, we could calculate critical angles, we found that all these transmitted signals existed in the experiment, shown in fig 7(a).

Fig 7a and 7b present magnitude spectra of S_{ij} comparisons between the microchannel with and without deionized water. The data evaluate whether and when the acoustic wave transmitted through the microchannel. There are seven sections of path of acoustic beam in the microsystem. The acoustic path of transmitted signal is labeled in fig 6 (path $\,$ I -path $\,$ VII).

The distances between the top of the mirrors and between transducers are the same as previously. The distance between the incidence point of the acoustic wave on the mirror and the vertical mirror is $125\mu m$. The width of the microchannel is $50\mu m$. The distance between the two vertical mirrors is $330\mu m$. A continuously sinusoidal wave was used as excitation.

As the limitation of the deposition condition, the SiO₂ thickness of vertical mirrors can not be well controlled, as a consequence mode conversion happened. The LLSLLLL represents that the longitudinal acoustic wave emitted by the transducer was reflected as longitudinal one by the first 45° mirror, the longitudinal wave was converted into shear wave by first vertical mirror and the shear wave was converted again into longitudinal wave by the second vertical mirror. Then the longitudinal wave went through the microchannel full with EDI water, finally remained as the longitudinal wave reflected by the second 45° mirror. In fig 7a, we can see good signal to noise ratio by comparison of the two situations in the microchannel. With empty channel the amplitude of S21 transmission signal due to parasitic acoustic signal is evaluated at 9.3×10-7 at around LLSLLLL propagation time while channel full with EDI water the amplitude of the peak is 2.7×10-5. Even if the absolute amplitude of the transmitted signal is lower than that in the configuration without vertical mirrors, the signal to noise ratio is greatly improved. The S/N increased to 29. We can use the strongest peak as the testing signal to characterize liquid properties or achieve particle detection.

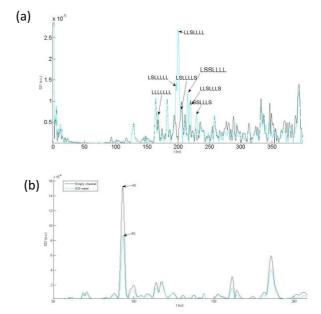


Fig 7 Real part of the impulse response of the system vs. time (ns): (a) S_{21} , (b) S_{22} (blue curve: channel full with EDI water; black curve: empty channel)

4. Conclusion

We presented a straightforward, inexpensive system for characterization and detection in microfluidic devices which will widen the applicability of BAW transducer applications. We realized the characterization by transmission through microchannel. Thanks to vertical mirrors integration, the signal to noise ratio for the peak of interest through the microchannel has been multiple by 26. Based on this kind of microsystem, ultrahigh frequency acoustic waves can be used to characterize and detect a variety of chemical and biological objects.

Acknowledgement

The authors would like to thank the support from the CNRS for international program for scientific collaboration (PICS). Jiaming Gao was supported by a fellow ship from the China Scholarship Council. The authors would like to thank all the staffs from the clean room and characterization room in IEMN

References

- [1] M. Hoummady, A. Campitelli, W. Wlodarski, *Smart Mater. Struct.* 6 (1997) 647.
- [2] R. Lucklum, P. Hauptmann, Meas. Sci. Technol. 14 (2003) 1854.
- [3] W.J. Grate, S.J. Martin, R.M.White, *Anal. Chem.* 65 (21) (1993) 940A.
- [4] S. Shiokawa, J. Kondoh, Jpn. J. Appl. Phys. 43 (2004) 2799 – 2802.
- [5] H. Wohltjen, et al., Acoustic Wave Sensor—Theory, Design, and Physico-Chemical Applications, Academic Press, San Diego, 1997, p. 39.
- [6] G.L. Cote, R.M. Lec, M.V. Pishko, *IEEE Sens.* J. 3 (2003) 251 266.
- [7] L.A. Kuznestsova, W.T. Coakley, *Biosens*. *Bioelectron*. 22 (2007) 1567 1577.
- [8] F.R.R. Teles, L.P. Fonseca, *Talanta* 77 (2008) 606 623.
- [9] Auld B. A. 1990 Acoustic Fields and Waves in Solids,2nd Edition, Vol II, Krieger Publishing Company
- [10] S. Wang, J. Gao, J. Carlier, P. Campistron, *Ultrasonics*, 51,5(2011), 532-538
- [11] S. Wang, J.CARLIER, P. CAMPISTRON, 9th Anglo-French Physical Acoustics Conference, AFPAC 2010, Lake District, UK, january 18-22, 2010